RSC Advances

PAPER

Cite this: *RSC Adv.*, 2022, **12**, 27300

Sandwich structure Aloin-PVP/Aloin-PVP-PLA/PLA as a wound dressing to accelerate wound healing

Weiping Li,†[a] Jingyu Wang,†[b] Zhiqiang Cheng,[a] Guixia Yang,*[a] Chunli Zhao,*[c] Feng Gao,[d] Zhongkai Zhang[d] and Yinjie Qian[d]

Received 10th April 2022
Accepted 12th July 2022

DOI: 10.1039/d2ra02320b

rsc.li/rsc-advances

We have prepared a new type of Aloin/Polyvinylpyrrolidone (PVP)-Aloin/PVP/polylactic acid (PLA)-PLA sandwich nanofiber membrane (APP), to achieve a time-regulated biphasic drug release behavior, used for hemostasis, antibacterial activity and accelerated wound healing. We tested the water absorption capacity, water contact angle, tensile strength, thermogravimetric analysis, Fourier transform infrared spectroscopy and *in vitro* drug release of the prepared material, as well as analyzed the morphology of the nanofiber membrane with a scanning electron microscope. In the wound healing experiment, the wound healing rate of APP on the 15th day was 96.67%, and it demonstrated excellent antibacterial activity by the disc diffusion method, showing superior antibacterial activity against Gram-negative bacteria. The skin defect model on the back of mice showed that APP nanofibers significantly induced granulation tissue growth, collagen deposition and epithelial tissue remodeling. Current research shows that the prepared composite nanofibers can quickly stop bleeding and can effectively promote wound healing.

1 Introduction

Skin plays an important role in protecting the body from external environmental interference such as pathogens and chemicals.[1] In our daily life, once the structure or function of the skin is defective, the body will be susceptible to microbial invasion and wound infection, which will delay wound healing to a certain extent, and may even be life-threatening.[2] Skin trauma, as a problem that cannot be ignored in global public health, has always been the focus of clinical treatment.[3] Healing is a complex process, which consists of four consecutive physiological stages, followed by wound bleeding, inflammation, cell proliferation and tissue remodeling.[4–6] The role of wound dressings includes the following steps: absorbing exudate, permeating oxygen, protecting the wound from infection, healing the wound, and maintaining a moist wound environment. While accelerating wound healing at a reasonable cost, they should also minimize patient discomfort.[7–9]

A wound dressing based on Aloin is developed, which is a natural biological material and bioactive compound. Aloe contains multiple compounds, and the types of compounds are more than 75 different compounds,[10] including vitamins (vitamins A, C, E and B12), enzymes (*i.e.* amylase, catalase and peroxidase), hormones (auxin and gibberellin) and others (*i.e.* salicylic acid, lignin and saponins) minerals (*i.e.* zinc, copper, selenium and calcium), sugars (monosaccharides such as mannose-6-phosphate and polysaccharides such as glucomannan[11]), (aloin and emodin), fatty acids (*i.e.* lupeol and campesterol), Therefore, Aloin has anti-inflammatory, antibacterial, anti-oxidant and wound healing properties[12,13] Whereas, the low elongation, elasticity and water absorption capacity of Aloin severely limit its use in wound dressings. Therefore, it is important to improve the mechanical properties of Aloin to broaden its potential applications.

PLA is a renewable polymer with cytocompatible, biodegradable, biocompatible properties extracted from corn, wheat, sugar beet and other plants,[14,15] it is cheap and easy to obtain.[16] Based on the above advantages, PLA is considered to be one of the most promising environmentally friendly polymer matrices in the context of sustainable development.[17–19] By blending with PLA, the mechanical properties of Aloin are greatly improved. PVP as a hydrophilic biocompatible polymer, has many functions like detoxification, hemostasis, increased dissolved concentration, prevention of peritoneal adhesions and promotion of blood sedimentation.[20–22] Due to its hydrophilic properties, PVP fiber can also be used as a fast-dissolving drug system, which helps to improve the dissolution profile of poorly water-soluble drugs and can be used for oral administration.[23] Electrospinning nanofiber membranes show excellent performance when they are used in wound dressings.[24–26] These

[a]College of Resources and Environment, Jilin Agriculture University, Changchun 130118, People's Republic of China. E-mail: 9677667@qq.com

[b]Jilin Academy of Agricultural Sciences, Changchun 130119, People's Republic of China

[c]College of Horticulture, Jilin Agricultural University, Changchun 130118, People's Republic of China. E-mail: zcl8368@163.com

[d]College of Plant Protection, Jilin Agricultural University, Changchun 130118, People's Republic of China

† These authors contribute to the work equally.

dressings have ductility and tensile strength comparable to human skin, so they can fit the wound well.[27] Meanwhile, the electrospinning nanofiber membrane also has the characteristics of the three-dimensional support structure, small pore size and high surface area to volume ratio.[28] To a certain extent, the designed electrospinning nanofiber membranes can be used to simulate the biological functions of extracellular matrix (ECM) and provide an ideal microenvironment for cell adhesion, proliferation and further differentiation.[29]

In this work, we prepared a new sandwich-like nanofiber membrane (APP) using the sequential electrospinning method, which is loaded with Aloin thus can help accelerate wound healing. The first layer is composed of Aloin and PVP as a hemostatic agent. This layer of nanofiber membrane plays a role in quickly stopping bleeding, absorbing exudate and keeping the wound moist. The middle layer is composed of Aloin/PVP/PLA. The hydrophobicity of PLA can make the fiber membrane achieve the purpose of drug release and reduce wound oxidative stress and inflammation. In addition, the outermost layer is composed of PLA, which isolates the external environment, prevents bacteria from attaching, and avoids wound infection. The prepared multilayer structure is expected to coordinate the function of the membrane module corresponding to the healing stage and accelerate the healing process at the same time.[30]

2 Materials and methods

2.1 Materials

Polyvinylpyrrolidone (PVP, molecular weight = 630 kDa) was purchased from Okem Chemical Technology Co. Ltd (Guangzhou, China). Polylactic acid (PLA 3051D) was purchased from NatureWorks. *N,N*-Dimethylformamide (DMF), chloroform ($CHCl_3$) and 75% absolute ethanol (C_2H_5OH) were purchased from Beijing Chemical Plant. Aloin (95% purity) was purchased from Xi'an Yunrui Biotechnology Co. Ltd Deionized water comes from our laboratory.

2.2 Preparation of fiber membrane

Dissolve 10 wt% PVP and 5 wt% Aloin in 75% ethanol (C_2H_5OH) as the first layer of the sandwich structure; dissolve 10 wt% PVP and 5 wt% Aloin in 75% ethanol on both sides of the roller. And 10 wt% PLA is dissolved in DMF and $CHCl_3$ (1 : 4w/w) to receive the nanofiber membrane in both directions as the middle layer of the sandwich structure; 10 wt% PLA is dissolved in DMF and $CHCl_3$ (1 : 4 w/w), as the third layer of the sandwich structure. Through investigation, we found that when the voltage is 17 kV at room temperature and the distance between the needle tip and the roller is 12 cm, the PVP nanofiber membrane with Aloin is smoother, which makes the antibacterial experiment part more effective. All the prepared samples were stirred in a water bath at 30 °C for 24 hours to obtain a homogeneous solution. When the voltage is 11 kV and the distance between the needle tip and the drum is 12 cm, the electrospun PLA nanofiber membrane spins more uniformly and the effect is better. Finally, the composite nanofiber mat was placed in an oven at 35 °C and vacuum dried for 24 hours to fully remove residual solvents, and the samples were used for further characterization.

2.3 Bidirectional electrospinning

In order to co-spun hydrophobic PLA and hydrophilic PVP, we utilize the two-way spinning method. Through one drum, two voltages, and two electrospinning solutions, bidirectional electrospinning realizes the uniform fusion of hydrophobic and hydrophilic nanofiber membranes. The two voltages independently control their corresponding spinning solutions, this makes the resulting nanofiber membrane smooth and flat. The two-way electrospinning method improves the hydrophilicity (hydrophobicity) of the nanofiber membrane, consequently, the drug release rate is controlled, and the subsequent drug release is provided.

2.4 Preparation of three-layer wound accessories

The three-layer wound dressing, or sandwich structure, uses the drug-loaded hydrophilic layer as the first layer, which is the rapid drug's release layer; the nanofiber membrane obtained by bidirectional electrospinning is used as the middle layer, which is the drug slow-release layer; the hydrophobic layer serves as the third layer, which is the external insulation layer. After optimizing the electrospinning conditions, the preparation was carried out in three steps: (i) PVP-loaded Aloin nanofibers were electrospun for 2 hours as the first layer as the drug rapid release layer; (ii) PVP-loaded Aloin and PLA was used as the middle layer was electrospun for 2 hours as the slow release layer of the drug; (iii) Finally, the PLA nanofibers were electrospun for 2 hours as the isolation layer of the drug. The sandwich structure combines a drug immediate-release layer + a slow-release layer + an insulating layer, the structure of which makes it have a better antibacterial effect, and is an effective application of electrospinning nanofiber membrane in skin wound dressings in the future.

2.5 Characterization of nanofiber membranes

The morphology and diameter of the prepared fibers were characterized by scanning electron microscopy (SEM, SHIMADZU S-550). The diameters of the nanofibres were recorded and calculated for 100 randomly selected nanofibres from the images by means of Image J software. FTIR-650 was used to analyze the bonding structure of the samples and the interactions between different parts of the nanofibers. The Fourier transform infrared spectrum ranges from 4000 cm^{-1} to 400 cm^{-1}. The mechanical properties are measured with a universal testing machine (WDW-100, Shandong Bang Testing Machine Co. Ltd. China) at a tensile speed of 15 mm min^{-1}. According to ASTM Standard 638, the sample is made into a standard dumbbell shape by die-cutting from the prepared mat. When testing in the longitudinal direction, record the tensile strength and elongation at break of each sample. The wettability is measured by using the contact angle of deionized water (Shanghai Solon/China SL200KS). The deionized water is automatically injected, the sample reference surface and the

needle position are set, and the stop drop method is used for testing. A differential scanning calorimeter (1100LF, METTLER, Switzerland) was also used to study the thermodynamic properties of the prepared nanofibers. The prepared nanofibers were placed in a pot and heated to 900 °C. The initial temperature of the instrument is 25 °C and the heating rate is 10 °C per minute.

2.6 Water absorption test

The wound body fluid is made of PBS buffer. Weigh the initial weight (W_o) of the dry nanofiber membranes; then float them in PBS (temperature = 37 °C) for 24 hours, weigh them after soaking (weight), and record them as W_t. The test was repeated three times for each sample ($n = 3$). The degree of water absorption is calculated according to the following formula.[8,31]

$$\text{Water uptake (\%)} = W_t - W_o/W_o \times 100\%$$

2.7 Antibacterial experiment

The antibacterial activity of the electrospinning nanofiber PVP/Aloin + PVP/Aloin and PLA + PLA sandwich structure was detected by the inhibition zone method. In this study, Gram-positive *Staphylococcus aureus* and Gram-negative *Escherichia coli* were selected as model microorganisms. All bacterial cultures come from the laboratory. First configure the solid medium, isolate and purify the strains, then use the liquid medium to culture in a shaker at 37 °C for 24 hours. When the conical flask appears turbid, it means that a new generation of bacterial liquid has been cultivated. Use a pipette to measure 100 μL Add dropwise to the plate, and paste the bacteriostatic material on the plate containing the bacteriostatic liquid. Paste 3 identical bacteriostatic materials on each plate, that is, 3 replicates, and incubate in a 36 ± 1 °C incubator for 48 hours. We observed bacterial growth on the plate, but no bacteria in the area where the antibacterial material was attached, and an obvious inhibition zone was formed around it. The antibacterial performance of the material is evaluated by measuring the diameter of the inhibition zone.

2.8 *In vitro* drug release studies

In order to study the drug release behavior of Aloin-loaded wound dressings, the nanofibers were weighed 0.0211 g and placed in a PBS solution (15 mL, pH = 7.4); then, within a specific time, 500 μL of each sample was extracted, and then UV-visible Spectrophotometer (T6 New Century, Beijing Purkinje General Instrument Co. Ltd) detects the release of Aloin at $\lambda_{max} = 323$ nm. After that, in order to keep the conditions as unchanged as possible, the solution was replaced with a fresh PBS solution of the same volume as the release medium. After repeating the test 3 times on all samples, report the average drug release. A calibration curve was used to calculate the cumulative drug release in PBS. Plot the cumulative Aloin release curve based on time. The calibration curve is based on the release amount of Aloin in PBS: $y = -79.906 + 33.703(1 - \exp(-X/74.978)) + 145.067(1 - \exp(-X/3.566))$, $R^2 = 0.9991$.

2.9 Wound healing in the body

In the wound healing experiment, healthy male mice weighing 20 ± 3 g were used. All animal studies were conducted with guidelines approved by the Animal Experiment Ethics Committee of Jilin Agricultural University. Divide the mice used in the experiment into four groups, which are the control group, low concentration group, medium concentration group, and high concentration group. After the mice were anesthetized with 4% chloral hydrate (0.01 mL g^{-1}), the back was scraped off with a blade and disinfected with 70% ethanol. Then mark a circle with a diameter of 1 cm on the back of the rat, and use sterile scissors to cut off the marked area of the skin on the back of the mouse. Regularly (0, 2, 4, 6, 8, 10, 12, and 14 days) take pictures of the wound and record its area. The percentage of wound area is calculated by the following equation:

$$\text{Wound closure (\%)} = S_o - S_n/S_o \times 100\%$$

S_o is the area of the original wound and S_n is the area of the actual wound (on the 5th, 10th and 15th days after the injury). On the 5th, 10th, and 15th days after treatment, the mice in each group were euthanized for histological analysis.

2.10 Histological analysis

The wound tissues on 5, 10, and 15 days after surgery were kept overnight in 4% paraformaldehyde in 0.01 M PBS (PH = 7.4) and embedded in paraffin. Using a paraffin microtome (Leica M2235), to cut the paraffin into sections with a thickness of 5 microns and stained with hematoxylin-eosin and Masson trichrome.[32] A Zeiss Axio microscope was used to observe the tissue sections.

3 Results and discussion

3.1 Particle size analysis

Image analysis software (ImageJ, version 1.65) was used to measure the average diameter of nanofibers from SEM micrographs. Randomly select 100 fibers in each SEM image of the corresponding sample for evaluation to obtain the average diameter. The thickness of the prepared PLA, Aloin/PVP-PLA, and Aloin/PVP nanofibers were 0.0655 mm, 0.073 mm, and 0.893 mm, respectively. They are placed on the bottom, middle and upper layers of the sandwich structure, respectively. Although the spinning time of PLA solution is longer, the second and third layers of Aloin-loaded nanofiber membranes are thicker than PLA nanofibers due to the higher concentration of the spinning solution. By controlling the solution concentration and spinning time, the thickness of the membrane is controllable, so the "sandwich" structure can freely adjust the amount of drug release and the duration of release. The morphology of the three kinds of nanofibers presents a random orientation, a bead-free structure and a smooth surface. The average diameter of sandwich structure nanofibers is 1.41 μm, the average diameter of PLA nanofibers is 1.74 μm, the average diameter of PLA/PVP-Aloin nanofibers is 1.45 μm, the average diameter of PVP-Aloin nanofibers is 1.46 μm, and the average

diameter of PLA nanofiber membranes is 1.4 μm (Fig. 1). The diameter is much larger than the average diameter of the loaded Aloin nanofiber membrane, which shows that Aloin has excellent compatibility and is evenly distributed in the nanofiber membrane. Compared with the average diameter of the pure PLA nano-fiber membrane, with the addition of Aloin, the average diameter of the nanofiber membrane is greatly reduced and the specific surface area is increased. This is extremely conducive to the application of wound dressings. It is noteworthy that during the electrospinning process there was no aggregation of Aloin on the surface due to phase separation. This means that the drug has good compatibility with the polymer solution, which is essential to prevent the initial rupture and release of the drug, thereby forming high-quality nanofibers. Next, further study the compatibility of the drug in the polymer solution by FTIR analysis. Interestingly, PVP/Aloin + PLA nanofibers show an unexpectedly flat shape, while PVP/Aloin nanofibers show a rare fritter-like structure. Besides, this is the first uniaxial electrospinning of PVP and Aloin nanofibres. We analyzed that the reason for the formation of the fritter-like structure may be due to the viscosity and surface tension between the solutions or the complex chemical reaction between Aloin and PVP.

3.2 Thermogravimetric analysis

The thermal stability of the composite nanofiber membrane was evaluated by TGA. Fig. 2 shows the TGA curves of the control PLA, PVP-Aloin, PLA/PVP-Aloin and PLA/PVP-Aloin/PVP-Aloin-PLA nanofiber membranes. The initial decomposition temperature of PVP-Aloin and PLA/PVP-Aloin nanofiber membranes is 230 °C, and the initial decomposition temperature of PLA/PVP-Aloin/PVP-Aloin-PLA nanofiber mats is 235 °C. The initial decomposition speeds of the three are very close. And it is much lower than the decomposition temperature of the control PLA at 280 °C, which indicates that the addition of Aloin reduces the initial decomposition temperature of the polymer itself, indicating that the thermal stability of Aloin in the composite nanofibers is low. It can be seen from the curve that the sandwich structure nanofiber membrane exhibits a single-stage degradation, which fully reflects that the composite nanofiber has better thermal stability.

3.3 FTIR

Characterize the intermolecular interactions of physical mixtures by FTIR.[33] Aloin/PVP, Aloin/PVP and PLA, PLA and their three sandwich structure nanofiber membrane spectra are shown in Fig. 3, Aloin/PVP, Aloin/PVP, PLA, PLA and their sandwich structure are all in 3300–2800 cm^{-1}, 1675–1640 cm^{-1}, 1600–1450 cm^{-1}, 1200–1000 cm^{-1} area, respectively, corresponding to C–H stretching vibration absorption, C=C stretching, C=C frame vibration and C–O stretching vibration. It can be seen that Aloin/PVP, Aloin/PVP and PLA, PLA and all the characteristics of the sandwich structure that constitute the peaks are all visible, and some peaks overlap. Due to the relative similarity and mobility of PLA and PVP drug-loaded nanofibers, most of the PLA, PVP and Aloin peaks have overlapped. Compared with the original PLA, the peak intensity was observed to decrease with the addition of PVP and Aloin. This may be attributed to the formation of hydrogen bonds between

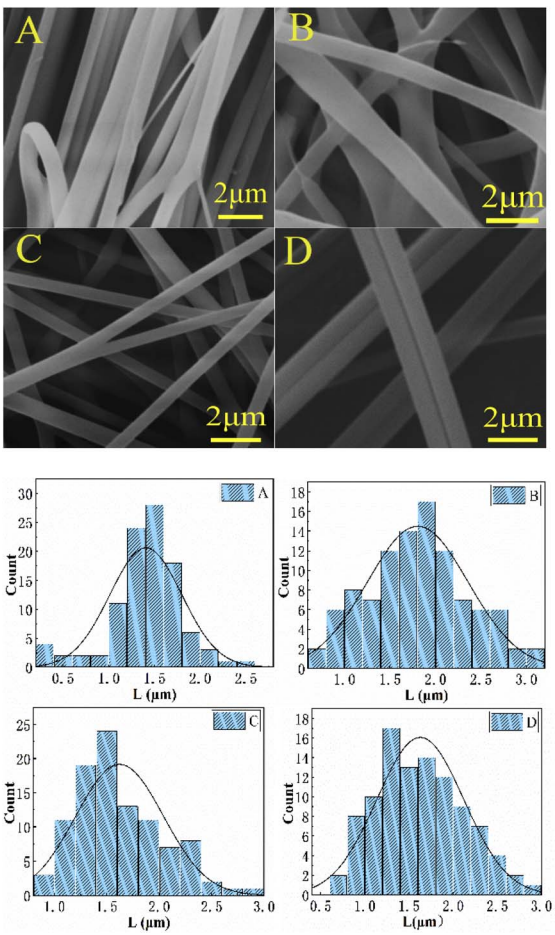

Fig. 1 Is a scanning electron microscopic photo and diameter distribution diagram of the scanning electron microscopic photo and diameter of the mezzanine structure, insulation layer, slow release layer, fast-release layer, fast-release layer A, B, C, and D.

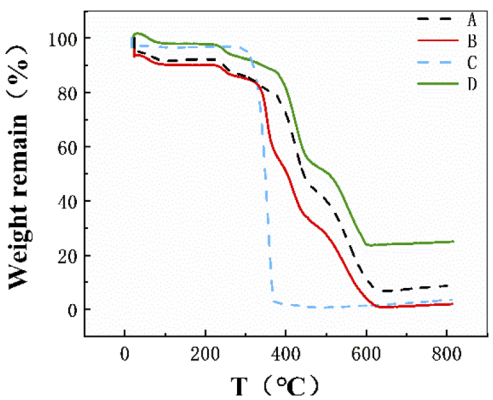

Fig. 2 Shows the thermogravimetric analysis diagrams of sandwich structure, insulation layer, slow release layer, and quick release layer A, B, C, and D in sequence.

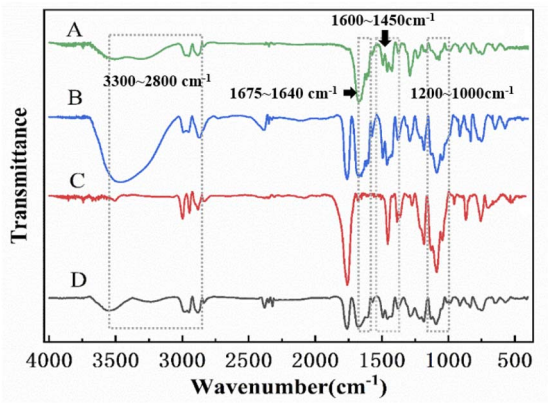

Fig. 3 Shows the infrared analysis diagrams of sandwich structure, insulation layer, slow release layer, and quick release layer A, B, C, and D in turn.

components, and compared with the hydrogen bond between the same polymer, two different macromolecules will form a stronger hydrogen bond.[34] Besides, it has been reported that the hydrogen bond between PLA, PVP and Aloin is easy to form. Therefore, FTIR confirmed the blend of PLA, PVP and Aloin.

3.4 Stress–strain curve

Fig. 4 shows the elongation at break and mechanical strength curves of the composite electrospinning membrane. The mechanical properties of wound dressing materials are considered important as an important evaluation index, because these materials require a certain degree of tensile strength, flexibility and good elasticity during handling and replacement. Sander *et al.* reported that the tensile strength of human skin is about 1–40 MPa,[35] which is similar to the tensile strength of our wound dressings. Fig. 4(A) shows a sandwich structure with a three-layer structure, which shows staged mechanical strength and flexibility. In order to achieve a reasonable balance of flexibility and hardness, it can be achieved by mixing a certain proportion of PVP and Aloin. In Fig. 4(B), compared with sandwich composite nanofibers, pure PLA has better elasticity and strength. Fig. 4(C) shows the bidirectional spinning PVP/Aloin/PLA.

Due to the addition of PLA, the mechanical properties of the material are improved. Fig. 4(D) stands for the nanofiber membrane of PVP/Aloin. Compared with conventional wound treatment materials, the soft nanofiber membrane is easier to handle and easy to peel and replace from the wound site, so it can withstand the pressure of different contours of different parts of the body.[23] Therefore, the composite nanofiber material has good air permeability and elasticity, and can be used as a wound dressing material.

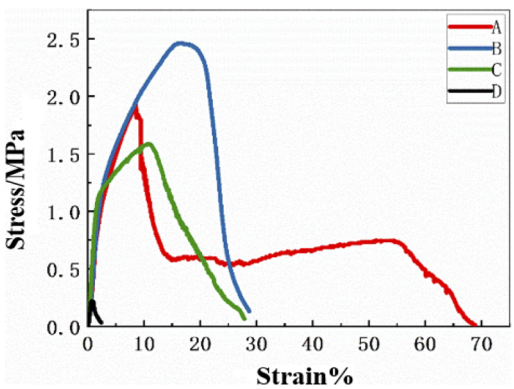

Fig. 4 Shows the stress–strain curves of sandwich structure, insulation layer, slow release layer, and quick release layer A, B, C, and D in sequence.

3.5 Contact angle

The contact angle measurement details of the composite nanofibers are shown in Fig. 5. As shown in Fig. 5(A), the PLA nanofibers in the insulating layer exhibit hydrophobicity, with a contact angle of approximately 126.1 ± 2°. As shown in Fig. 5(C), through bidirectional electrospinning, as PVP/Aloin is added to the other side of the drum, the contact angle has a way of transforming the composite nanofiber to hydrophilicity. The contact angle has changed from the original hydrophobic to hydrophilic. However, the contact angle in the "sandwich" structure is basically the same as the contact angle of the insulating layer of purely spun PLA, as shown in Fig. 5(B). This is because we put the insulating layer on the first layer when measuring the contact angle, making the "sandwich" structure of nanofiber membranes have the same contact angle as purely spun PLA, showing hydrophobicity, which is like wrapping hydrophilic drugs with hydrophobic nanofiber membranes to protect the drugs and isolate the outside world. As shown in Fig. 5(D), Aloin-loaded PVP has strong super-hydrophilic properties. This is because both PVP and Aloin are hydrophilic substances, which facilitate the burst release of drugs to achieve rapid hemostasis and anti-inflammatory effects. In contrast to our work, a more hydrophilic nanofiber surface will help cell attachment,[33] but may result in poor fiber stability. Therefore, the "sandwich" structure of electrospinning combines the hydrophobic polymer and the hydrophilic polymer better to maintain good surface wettability and fiber-forming properties.

3.6 Water absorption capacity

The solubility of fiber membrane in water will affect its own water absorption. After immersing APP in PBS for 24 hours, the water absorption reached 159%. This may be attributed to the presence of hydrophilic groups, such as the hydroxyl group in

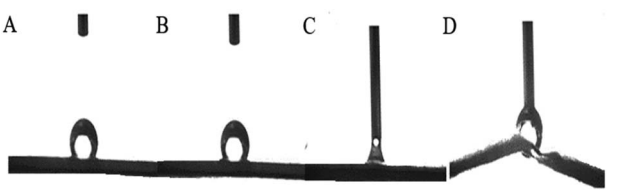

Fig. 5 Shows the contact angles of A, B, C, and D are sandwich structure, insulation layer, slow release layer, and quick release layer in turn.

Aloin and the lactam of PVP. Hydrophilic groups form hydrogen bonds with water molecules, increasing water absorption capacity. The good water absorption capacity of the wound dressing will cause the absorption of excess wound exudate and help the wound water balance.[36]

3.7 Antibacterial test of composite nanofiber

Aloin is a compound with antibacterial activity against *Staphylococcus aureus* and *Escherichia coli*. It acts by inhibiting the formation of biofilms and the production of extracellular proteins.[37] We use a puncher to punch PVP/Aloin, PVP/Aloin-PLA and PVP/Aloin-PLA into wafers of the same size, and place them on a clean operating table for 12 h ultraviolet sterilization. To be used, make three discs for each material, that is, 3 repetitions. Finally, place the discs on a plate dripped with *Escherichia coli* and *Staphylococcus aureus*. After culturing in a 37 °C incubator for 48 hours, the size of the inhibition zone was measured. The longer the diameter of the inhibition zone, the better the antibacterial effect. As shown in Fig. 6, the nanofiber membrane loaded with Aloin has strong antibacterial properties, especially for *Escherichia coli*, the antibacterial effect is better. Interestingly, the PVP/Aloin discs formed antibacterial after 24 h in the incubator circle, this further shows that its drug burst release can quickly release the drug in a short time to achieve antibacterial and anti-inflammatory effects, and PVP/Aloin-PLA and PVP/Aloin-PLA are all after 48 h. The zone of inhibition reaches the maximum, indicating that the drug has a slow-release effect, that is, the fast-release layer releases the drug the first time to deal with skin damage, and the slow-release layer gradually releases the drug, that is, slowly releases the effective drug to achieve healing. The last isolation layer is a safety protective layer, which ensures the whole process of skin healing.

3.8 *In vitro* drug release test of composite nanofibers

In this study, the high drug loading efficiency is caused by the same hydrophilicity of the drug and polymer, which is similar to the research results of Chogan *et al.* and Hadjianfar *et al.*, and this phenomenon is conducive to the best interaction between the polymer and the drug, which is conducive to the optimal interaction between the polymer and the drug.[38,39] In this experiment, the first-order kinetic equation, LangevinMod equation, and expAssoc equation are respectively fitted. R^2 are respectively: 0.8830, 0.9062, 0.9990. The nanofibers showed 60.49% drug release in the first 10 minutes, confirming the initial explosive release behavior in the first 10 minutes, which is the main focus of the production of drug carriers. The above results are closely related to the hydrophilicity of PVP, because it accelerates the release rate of the drug in the fiber membrane in the initial stage.[40] The high hydrophilic character causes the polymer–solvent interaction to increase, and the rapid absorption of the solvent will cause the volume of the polymer matrix to increase to a certain extent, which will eventually cause the polymer chain to become loose from its helical structure.

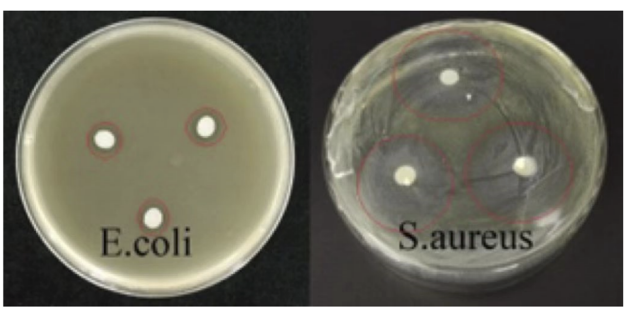

Fig. 6 Shows the antibacterial ability of sandwich nanofiber membranes against *Escherichia coli* and *Staphylococcus aureus*.

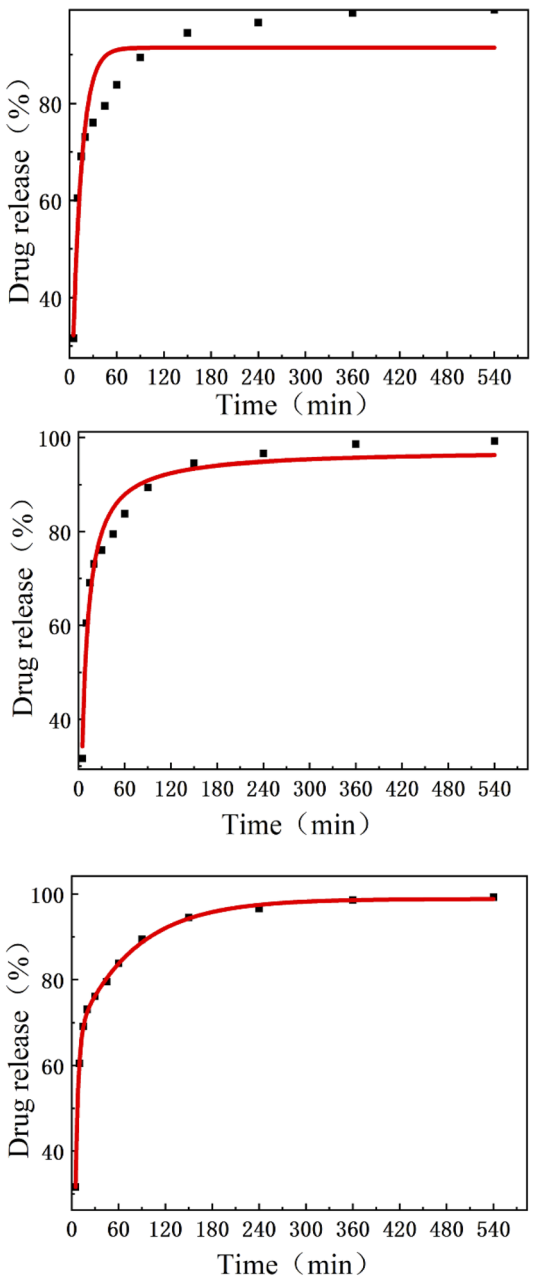

Fig. 7 Shows the first order dynamics, LangevinMod, ExpAssoc equations.

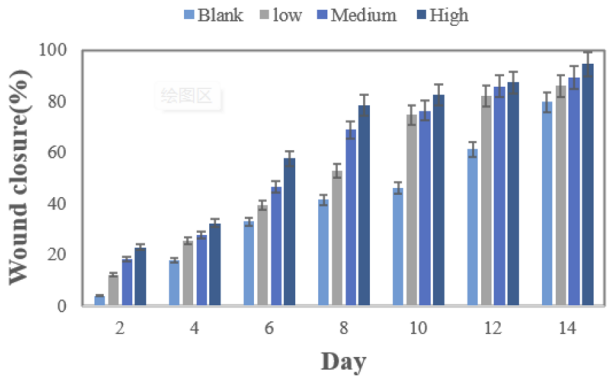

Fig. 8 Shows the wound healing rate of the blank group, low concentration, medium concentration, and high concentration.

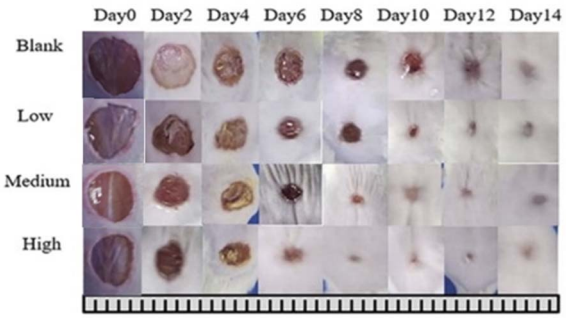

Fig. 9 Control wound healing photos, photos of low concentration, medium concentration, and high concentration nanofibers on 0, 2, 4, 6, 8, 10, 12, and 14 days.

The three-layer nanofibers show the composite release behavior of APP nanofibers, as shown in Fig. 7. The release curve of the three-layer nanofibers showed a sudden release within 10 minutes (60.49%), and then turned to a stable release within the next 9 hours. The cumulative release amount reached 99.28%, indicating that the drug initially experienced rapid release and then entered a slow release period. This release behavior is essential in the treatment of certain actual diseases. People always hope to relieve pain quickly after administration, and then extend the analgesic time through sustained release to provide long-term effects.[41] The release curve of the three-layer nanofiber can be described as the rapid release of the PVP nanofiber matrix in the initial stage, and the content of PLA delays the release of the three-layer system. We respectively fitted the first-order kinetics, LangevinMod, and ExpAssoc equations, and the R^2 obtained were 0.8937, 0.9062, and 0.9991, respectively. In summary, thanks to the simple sequential electrospinning and two spinning materials with different release behaviors, the three-layer nanofiber system can successfully achieve the dual-phase drug release behavior. Therefore, this novel nanofiber membrane can be used as a time-regulated drug release carrier.[23]

3.9 *In vivo* wound healing

The wound healing of mice was observed every two days. On day 14, compared with the control group, the wound treated with the prepared nanofiber scaffold showed better wound healing.[42] By day 6, the wound size of the animals treated in the blank group, low concentration group, medium concentration group, and high concentration group were reduced by 32.89%, 39.33%, 46.62%, and 57.72%, respectively. On the 14th day, the wound size of the four groups was reduced by 79.61%, 86%, 89.19%, 94.63% (Fig. 8), especially the high-concentration group. On the 8th day, the wound size was almost completely healed, indicating that the use of sandwiches containing Aloin structured nanofiber membrane has a positive effect on wound healing. As shown in Fig. 9, animals not treated with Aloin matrix showed mild redness, while animals treated with Aloin matrix did not show any visual signs of infection or inflammation. So we use tissue biopsy to analyze the wound healing degree of the four groups.

Fig. 10 shows that four groups of mice were sacrificed on the 5th, 10th and 15th day for the tissue analysis. On the 5th day, the sparse granulation tissue of the wound of the blank group showed inflammatory cells and neutrophils, which indicated severe inflammation. On the 10th day, inflammatory cells and neutrophils were significantly reduced, there were a small number of fibroblasts, and the granulation tissue at the wound gradually grew. On the 15th day, the wound showed inflammatory cells, macrophages, neutrophils and fibroblasts, and the upper fibroblasts were more intense. Compared with the blank group, the wound treated with APP nanofiber membrane showed a small number of inflammatory cells, macrophages, and neutrophils. Significantly, fibroblasts were not only dense but also evenly distributed. Among them, the high concentration of APP nanofiber membrane had an optimal wound healing effect.

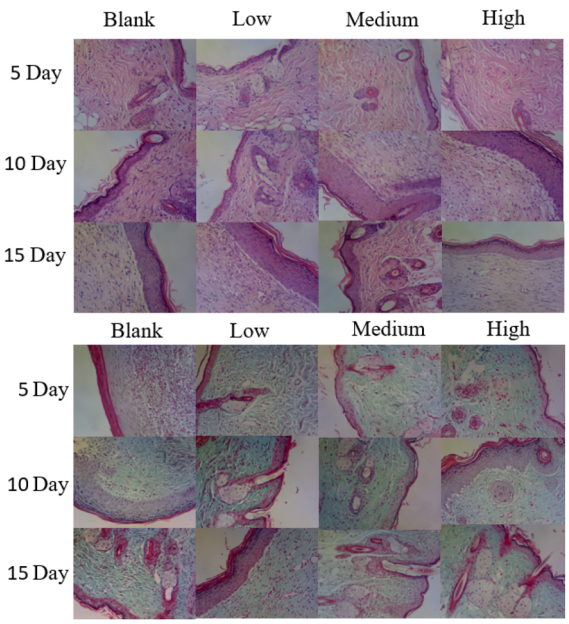

Fig. 10 HE staining (hematoxylin and eosin staining) and Masson's trichrome staining of skin tissue treated with nanofibers in the blank group, low concentration group, medium concentration group, and high concentration group. Microscope magnification = 100 times.

4 Conclusions

In this experiment, a three-layer nanofiber membrane of Aloin/PVP/PLA was successfully prepared by sequential electrospinning. Their morphology, chemical structure, water absorption, thermogravimetry, antibacterial activity and wound healing ability were investigated respectively. Scanning electron microscope (SEM) observed that the diameter of nanofibers is uniform and the surface is smooth. What is interesting is that the electron microscope image of PVP/Aloin is a typical "fritter-like" structure, which provides a reference for the next step in the application of catalytic oxidation, drug delivery, *etc.* The Fourier transform infrared spectroscopy shows that Aloe is dispersed at the molecular level in the polymer matrix; the contact angle shows that the first layer has a hydrophilic structure, the second layer is between hydrophilic and hydrophobic, and the third layer is a hydrophobic structure, indicating a "sandwich" overall membrane, the structure of which provides the possibility for the phased release of the drug; the stress–strain curve shows that the three-layer nanofiber mesh can compensate for the weak mechanical properties of the Aloe fiber by forming a three-layer grid with the strong PVP/PLA nanofiber matrix. The addition of PLA can control the sustained release of the drug. The Aloe added in the nanofiber can effectively inhibit the growth of Gram-positive bacteria and Gram-negative bacteria at the same time, with better antibacterial effects against Gram-positive bacteria than against Gram-negative bacteria. The drug-loaded nanofiber network exhibits a biphasic release behavior, first showing rapid drug release, followed by sustained release. At the same time, the drug release rate and sustained release behavior of the nanofiber membrane can be controlled by adjusting the spinning time and adjusting the thickness of the mesh. The sequential electrospinning technology successfully realized the time regulation of drug release. In a short time, the nanofiber membrane can stop bleeding immediately and then release the drug. *In vitro* wound healing studies have shown that APP nanofibers increase the wound healing rate and collagen deposition. In summary, this study provides a simple and feasible method for APP composite nanofibers for wound healing and preparation of a new three-layer drug-controlled release carrier, which is expected to become an effective wound dressing.

Ethics statement

All animal procedures were performed in accordance with the "Guidelines for the Ethics and Use of Laboratory Animals" of "Jilin Agricultural University" and were approved by the Animal Committee of "Jilin Agricultural University".

Conflicts of interest

There are no conflicts to declare.

Acknowledgements

This work was supported by the Jilin Province Innovation Capacity Building Fund Project (2020C024-5) and the Jilin Province Science and Technology Development Project (20200708066YY) B.

References

1 C. A. W. Choong, K. Y. Cheong, T. B. Keem, *et al.* Skin tissue engineering advances in severe burns: review and therapeutic applications, *Int. J. Burn. Trauma*, 2016, **4**, 3.
2 A. R. Unnithan, G. Gnanasekaran and Y. Sathiahkumar, Electrospun antibacterial polyurethane-cellulose acetate-zein composite mats for wound dressing, *Carbohydr. Polym.*, 2014, **102**, 884–892.
3 K. Sen Chandan, *et al.* Human skin wounds: a major and snowballing threat to public health and the economy, *Wound Repair Regeneration*, 2009, **17**, 763–771.
4 L. Ioanna, K. Ourania, A. Tone, *et al.* Collagen-Containing Fish Sidestream-Derived Protein Hydrolysates Support Skin Repair *via* Chemokine Induction, *Mar. Drugs*, 2021, **19**, 396.
5 O. Jiang, Q. Bu, N. Tao, *et al.* A facile and general method for synthesis of antibiotic-free protein-based hydrogel: Wound dressing for the eradication of drug-resistant bacteria and biofilms, *Bioact. Mater.*, 2022, **18**, 446–458.
6 S. Akita, Wound repair and regeneration: mechanisms, signaling, *Int. J. Mol. Sci.*, 2019, **20**, 6328.
7 Y. Liu, S. Zhou, Y. Gao, *et al.* Electrospun nanofibers as a wound dressing for treating diabetic foot ulcer, *Asian J. Pharm. Sci.*, 2019, **14**, 130–143.
8 T. MirmajidiI, F. Chogan, A. H. Rezayan, *et al. In vitro* and *in vivo* evaluation of a nanofiber wound dressing loaded with melatonin, *Int. J. Pharm.*, 2021, 596.
9 Biotechnology-Biopolymers; Findings from Koszalin University of technology yields new findings on biopolymers, (Biopolymers for Biomedical and Pharmaceutical Applications: Recent Advances and Overview of Alginate Electrospinning[J]). *Biotech Week*, 2019.
10 Sánchez, E. González-Burgos, I. Iglesias, *et al.* Pharmacological Update Properties of Aloe Vera and its Major Active Constituents, *Molecules*, 2020, **25**, 1324.
11 . Chabala, C. E. E. Cuartas and M. E. L. López, Release Behavior and Antibacterial Activity of Chitosan/Alginate Blends with Aloe vera and Silver Nanoparticles, *Mar. Drugs*, 2017, **15**, 328.
12 C. Palmer, T. Iamail, S. P. Lee, *et al.* Filaggrin null mutations are associated with increased asthma severity in children and young adults, *Allergy*, 2008, **120**, 64–68.
13 A. A. Maan, A. Nazir, M. Khan, *et al.* The therapeutic properties and applications of Aloe vera: A review, *J. Herb. Med.*, 2018, 1–10.
14 A. A. Yussuf, I. I. Massoumi and A. Hassan, Comparison of polylactic acid/kenaf and polylactic acid/rise husk composites: the influence of the natural fibers on the mechanical, thermal and biodegradability properties, *J. Polym. Environ.*, 2010, **18**, 422–429.
15 O. Gordobil, I. Egüés, R. Llano-ponte, *et al.* Physicochemical properties of PLA lignin blends, *Polym. Degrad. Stab.*, 2014, **108**, 330–338.

16 M. Ghozali, S. Fahmiati, E. Triwulandari, *et al.* PLA/metal oxide biocomposites for antimicrobial packaging application, *Polym.-Plast. Technol. Mater.*, 2020, **59**, 1332–1342.
17 W. Ouyang, H. Yong, H. Luo, *et al.* Poly(Lactic Acid) Blended with Cellulolytic Enzyme Lignin: Mechanical and Thermal Properties and Morphology Evaluation, *J. Polym. Environ.*, 2012, **20**, 1–9.
18 S. K. Pillai, S. S. Ray, M. Scriba, *et al.* Morphological and thermal properties of photodegradable biocomposite films, *J. Appl. Polym. Sci.*, 2013, **129**, 362–370.
19 . Courgneau, S. Domenek, R. Lebossé, *et al.* Effect of crystallization on barrier properties of formulated polylactide, *Polym. Int.*, 2012, **61**, 180–189.
20 J. Ding, J. Zhang, J. Li, *et al.* Electrospun polymer biomaterials, *Prog. Polym. Sci.*, 2019, **90**, 1–34.
21 S. Tabasum, A. Noreen, A. Kanwal, *et al.* Glycoproteins functionalized natural and synthetic polymers for prospective biomedical applications: A review, *Int. J. Biol. Macromol.*, 2017, **98**, 748–776.
22 M. Teodorescu, M. Bercea and S. Morariu, Biomaterials of PVA and PVP in medical and pharmaceutical applications: Perspectives and challenges-ScienceDirect, *Biotechnol. Adv.*, 2019, **37**, 109–131.
23 H. Lee, G. Xu, D. Kharaghnai, *et al.* Electrospun tri-layered zein/PVP-GO/zein nanofiber mats for providing biphasic drug release profiles, *Int. J. Pharm.*, 2017, **531**, 101–107.
24 D. Subhamoy and A. B. Baker, Biomaterials and nanotherapeutics for enhancing skin wound healing, *Front. Bioeng. Biotechnol.*, 2016, **4**, DOI: **10.3389/fbioe.2016.00082**.
25 Liu, S. Zhou, Y. Gao, *et al.* Electrospun nanofibers as a wound dressing for treating diabetic foot ulcer, *Asian J. Pharm. Sci.*, 2019, **14**, 130–143.
26 Fahimirad and F. Ajalloueian, Naturally-derived electrospun wound dressings for target delivery of bio-active agents, *Int. J. Pharm.*, 2019, **566**, 307–328.
27 X. Ji, R. Li, W. Jia, *et al.* Co-Axial fibers with Janus-structured sheaths by electrospinning release corn peptides for wound healing, *ACS Appl. Bio Mater.*, 2020, **3**, 6430–6438.
28 H. Li, C. Xin, W. Lu, *et al.* Application of Electrospinning in Antibacterial Field, *Nanomaterials*, 2021, **11**, 1822.
29 Lauro Lima, T. Bezerra Taketa, M. Masumi Beppu, *et al.* Coated electrospun bioactive wound dressings: Mechanical properties and ability to control lesion microenvironment, *Mater. Sci. Eng. C.*, 2019, **100**, 493–504.
30 K. Chen, H. Pan, J. Dongxu, *et al.* Curcumin-loaded sandwich-like nanofibrous membrane prepared by electrospinning technology as wound dressing for accelerate wound healing, *Mater. Sci. Eng. C.*, 2021, **127**, 112245.
31 C. Gsab, E. Med, C. Ghab, *et al.* Electrospun anti-inflammatory patch loaded with essential oils for wound healing – ScienceDirect, *Int. J. Pharm.*, 2020, **577**, DOI: **10.1016/j.ijpharm.2020.119067**.
32 R. Li, Z. Cheng, R. Wen, *et al.* Novel SA@Ca^{2+}/RCSPs core–shell structure nanofibers by electrospinning for wound dressings, *RSC Adv.*, 2018, **8**, 15558–15566.
33 A. R. Unnithan, G. Gnanasekaran, Y. Sathishkumar, *et al.* Electrospun antibacterial polyurethane-cellulose acetate-zein composite mats for wound dressing, *Carbohydr. Polym.*, 2014, **102**, 884–892.
34 V. González, C. Guerrero and U. Ortiz, Chemical structure and compatibility of polyamide–chitin and chitosan blends, *J. Appl. Polym. Sci.*, 2000, **78**, 850–857.
35 E. A. Sander, K. A. Lynch and S. T. Boyce, Development of the mechanical properties of engineered skin substitutes after grafting to full-thickness wounds, *J. Biomech. Eng.*, 2014, **136**, 051008.
36 Y. Shi, Y. Li, J. Wu, *et al.* A novel transdermal drug delivery system based on self-adhesive Janus nanofibrous film with high breathability and monodirectional water-penetration, *J. Biomater. Sci., Polym. Ed.*, 2014, **25**, 713–728.
37 H. Xiang, F. Cao, D. Ming, *et al.* Aloe-emodin inhibits staphylococcus aureus biofilms and extracellular protein production at the initial adhesion stage of biofilm development, *Appl. Microbiol. Biotechnol.*, 2017, DOI: **10.1007/s00253-017-8403-5**.
38 H. Mehdi, S. Dariush and V. Jal Eh, Polycaprolactone/chitosan blend nanofibers loaded by 5-fluorouracil: An approach to anticancer drug delivery system, *Polym. Adv. Technol.*, 2018, **29**(12), 2972–2981.
39 T. Mirmajidi, F. Chogan, A. H. Rezayan, *et al. In vitro* and *in vivo* evaluation of a nanofiber wound dressing loaded with melatonin, *Int. J. Pharm.*, 2021, 120213.
40 H. Yu, P. Yang, Y. Jia, *et al.* Regulation of biphasic drug release behavior by graphene oxide in polyvinyl pyrrolidone/poly(ε-caprolactone) core/sheath nanofiber mats, *Colloids Surf., B*, 2016, **146**, 63–69.
41 H. Murakami, M. Kobayashi, H. Takeuchi, *et al.* Utilization of poly(dl-lactide-co-glycolide) nanoparticles for preparation of mini-depot tablets by direct compression, *J. Controlled Release*, 2000, **67**, 29–36.
42 J. K. Choi, Ji-H. Jang, W.-H. Jang, *et al.* The effect of epidermal growth factor (EGF) conjugated with low-molecular-weight protamine (LMWP) on wound healing of the skin, *Biomaterials*, 2012, **33**, 8579–8590.